Research Article | Vol. 31, No. 24 / 20 Nov 2023 / Optics Express 40142
Optics EXPRESS

Ultrafast pump-probe spectroscopy via chirped-pulse up-conversion with dispersion compensation

RYO TAMAKI,[1,2,3] MASASHI SUZUKI,[2] SATOSHI KUSABA,[2] JUN TAKEDA,[2] AND IKUFUMI KATAYAMA[2,*]

[1] *Kanagawa Institute of Industrial Science and Technology (KISTEC), 705-1 Shimoimaizumi, Ebina 243-0435, Japan*
[2] *Graduate School of Engineering Science, Yokohama National University, 79-5 Tokiwadai, Hodogaya, Yokohama 240-8501, Japan*
[3] *tamaki-ryo-jv@ynu.ac.jp*
[*] *katayama-ikufumi-bm@ynu.ac.jp*

Abstract: In this study, ultrafast transient signals were detected on a single-shot basis using chirped-pulse up-conversion spectroscopy with dispersion compensation. Unlike in the conventional time-encoding technique using chirped pulses, distortion of the ultrafast waveform was reduced by applying dispersion compensation to the chirped probe pulses and using sum-frequency generation with the chirped readout pulses. The method was applied to terahertz time-domain spectroscopy and near-infrared pump–probe spectroscopy, providing ultrafast observations with an improved temporal resolution comparable to the transform-limited pulse durations. Terahertz waveforms, Kerr rotation signals, and phonon-polariton oscillations were measured accurately with no significant waveform distortion, thereby showing the proposed scheme to be promising for single-shot pump–probe spectroscopy in a wide range of spectroscopic applications.

1. Introduction

Time-domain information on femtosecond and picosecond timescales is fundamentally important for understanding the dynamic behaviors of materials. Among the spectroscopic methods for revealing the dynamics, single-shot time-domain spectroscopy enables the observation of ultrafast signals in a wide range of phenomena while avoiding multiple measurements; such phenomena include highly excited processes close to material breakdown, irreversible phase changes, chaotic dynamics, and photobleaching [1–10]. With single-shot time-domain spectroscopy, it is possible to detect the initial ultrafast dynamics triggered by excitation from a single laser pulse, something that is difficult to do using conventional pump–probe spectroscopy with a scanning translation stage.

The key to realizing single-shot ultrafast measurements is choosing an axis for encoding the temporal information. Noncollinear geometry of the pump and probe pulses [11–13] or diffraction of the probe by an echelon [14–18] will result in the time-domain signal being encoded into the spatial domain, thereby necessitating an imaging setup if the time-domain information is to be detected precisely. The other method for single-shot measurements, *i.e.*, chirped-pulse spectroscopy (or time encoding), is a useful technique in which the time-domain signal is encoded in the spectrum of the probe [19,20]. Consequently, only a spectrometer is needed to obtain the temporal information, thereby avoiding the need for such an imaging setup. However, the time resolution of conventional chirped-pulse spectroscopy is limited by the square root of the product of the pump and probe chirped-pulse widths [21]. Figure 1(a) shows the time resolution (red line) of conventional chirped-pulse spectroscopy using 100 fs pulses, where the gray region cannot be resolved. Furthermore, waveform distortion due to spectral interference occurs if

#504429 https://doi.org/10.1364/OE.504429
Journal © 2023 Received 7 Sep 2023; revised 23 Oct 2023; accepted 31 Oct 2023; published 10 Nov 2023

Optics EXPRESS

the transient signal is close to the time resolution [22,23], thereby making it difficult to obtain accurate waveforms on the ultrafast time scale. Although several methods have been proposed for retrieving accurate waveforms from distorted signals (*e.g.*, in-line spectral interferometry [24], digital time-domain holography [25], and phase diversity electro-optic sampling [26]), sophisticated signal post-processing is essential for retrieving terahertz waveforms, thereby limiting the range of applications of chirped-pulse spectroscopy.

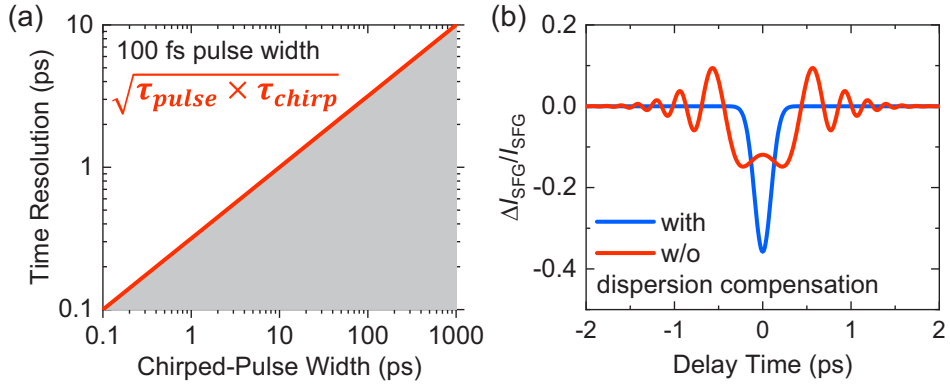

Fig. 1. (a) Time resolution of conventional chirped-pulse spectroscopy (red line) with 100 fs pulse width. The gray region cannot be resolved using the conventional method. (b) Simulation results for 200 fs Gaussian modulation with (blue) and without (red) dispersion compensation.

To overcome this issue, a novel technique has been proposed previously, *i.e.*, an up-conversion time microscope [27,28] using a time lens. Analogous to a conventional lens that magnifies an image spatially, a time lens magnifies a time-domain signal temporally, and it comprises two elements: (i) a component that yields group delay dispersion (GDD) and (ii) a quadratic phase modulation. The latter can be applied by electro-optic modulation [29], sum-frequency generation [27,28], or four-wave mixing [30]. By combining anomalous (negative) dispersion and sum-frequency generation, an up-conversion time microscope can encode a time-domain signal in the spectral domain without any distortion. The calculation results shown in Fig. 1(b) for the differential change in up-converted modulation signals ($\Delta I_{SFG}/I_{SFG}$) are for a 100 fs pulse width, a Gaussian modulation with a width of 200 fs, and a chirped-pulse width of ca. 5 ps. Without dispersion compensation, there is waveform distortion and reduced time resolution (red line), whereas performing sum-frequency generation between the dispersion-compensated probe pulse and the chirped readout pulse results in an accurate time-domain signal (blue line). Therefore, an up-conversion time microscope can retrieve accurate time-domain signals, but to the best of our knowledge, this technique is yet to be examined for ultrafast time-resolved measurements.

Herein, we demonstrate chirped-pulse up-conversion spectroscopy with dispersion compensation (combining time-encoding and time-lens techniques) applicable to detecting ultrafast transient signals with sub-picosecond time resolution on a single-shot basis. As shown schematically in Fig. 2, the signal distortion in conventional chirped-pulse spectroscopy originates from spectral interference between the chirped probe pulses and the ultrafast modulation signal. The ultrafast modulation waveform in the time domain (the blue line at the top left in Fig. 2) generates sideband signals (as indicated by the blue dashed ellipses in Fig. 2) that interfere with the original chirped probe pulses, resulting in an interference pattern in the frequency domain (the red line in Fig. 2). In the proposed scheme, anomalous dispersion is applied to the chirped probe pulse with time encoded modulation (top-right panel in Fig. 2). The dispersion of the chirped probe pulse is compensated by the anomalous dispersion, and the modulation signal is chirped negatively (blue

Optics EXPRESS

dashed ellipse). Then, another chirped pulse with the same dispersion as that of the chirped probe pulse is prepared as the readout pulse (bottom-right panel in Fig. 2). Finally, the sum-frequency signal between the dispersion-compensated probe pulse and the chirped readout pulse is generated to obtain up-converted modulation.

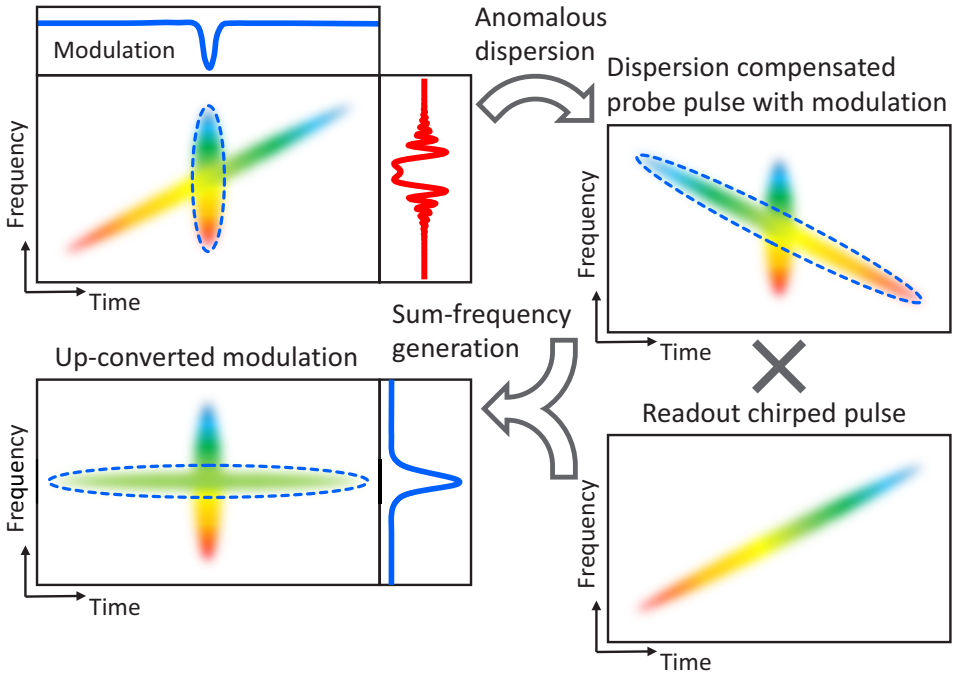

Fig. 2. Schematics of principle of chirped-pulse up-conversion spectroscopy with dispersion compensation. An ultrafast modulation signal is encoded to the chirped probe pulse, then anomalous dispersion is applied for dispersion compensation. Conversely, a chirped readout pulse is prepared, and finally sum-frequency generation is performed between the two pulses to obtain an up-converted modulation signal without waveform distortion.

The resultant sum-frequency signal shown in the bottom-left panel in Fig. 2 has encoded time-domain information in the spectral domain without distortion. The frequency of the modulation signal (blue dashed ellipse) is identical to the frequency sidebands of the chirped pulses, so no interference between the modulation signal and the probe pulse occurs in the frequency domain (the blue line to the right of the lower-left panel in Fig. 2). The modulated signal and the readout pulse must be chirped equally and oppositely to obtain the best result without distortion, *i.e.*, the aberration correction in the time domain.

2. Experimental setup

The optical setup is shown schematically in Fig. 3. A Ti:sapphire regenerative multi-pass amplifier was used as the femtosecond light source, and the pulse width, center wavelength, and repetition rate were 130 fs, 790 nm, and 1 kHz, respectively. Figure 3(a) shows the experimental setup for chirped-pulse up-conversion spectroscopy with dispersion compensation for terahertz time-domain spectroscopy. Terahertz pulses were generated by an organic N-benzyl-2-methyl-4-nitroaniline (BNA) crystal [31,32] excited by 2-μJ pump pulses. A Martinez pulse stretcher with a pair of gratings was used to generate chirped pulses, yielding an additive GDD of 0.4 ps^2, and the chirped pulse width was estimated to be 8.5 ps. The chirped pulses were split into two beams, one of probe pulses and the other of readout pulses. The probe pulses were used for phase offset

Optics EXPRESS

electro-optic (EO) sampling [33,34] using a 1-mm-thick ZnTe (110) crystal in the case of terahertz detection. Crossed-Nicols polarizers with a quarter-wave plate (QWP) were used to apply a small phase offset to achieve a good signal-to-noise ratio with small phase modulations [10,35]. A Treacy pulse compressor with a pair of gratings was used to apply an anomalous dispersion (GDD = −0.4 ps^2) to the modulated probe pulses, then sum-frequency generation between the probe and readout pulses was obtained by using a 0.5-mm-thick beta-barium borate (BBO) crystal in a noncollinear geometry. Finally, the up-converted signal was measured by a 50-cm spectrometer with a 2400 lines/mm holographic grating equipped with a 16-bit complementary metal oxide semiconductor (CMOS) linear sensor. The frame rate of the CMOS linear sensor was synchronized with the laser repetition rate of 1 kHz, and an optical chopper set at 500 Hz caused alternate excitation of the ZnTe crystal by the terahertz pulses. In the present setup, the positive and negative phase offset signals were measured alternately by rotating the QWP. Simultaneous measurements for the positive and negative phase offset signals were also performed to demonstrate real single-shot measurements as shown in Fig. 3(b). Terahertz waveforms were retrieved by considering the EO coefficient of the ZnTe crystal and the positive and negative phase offset angle of the QWP.

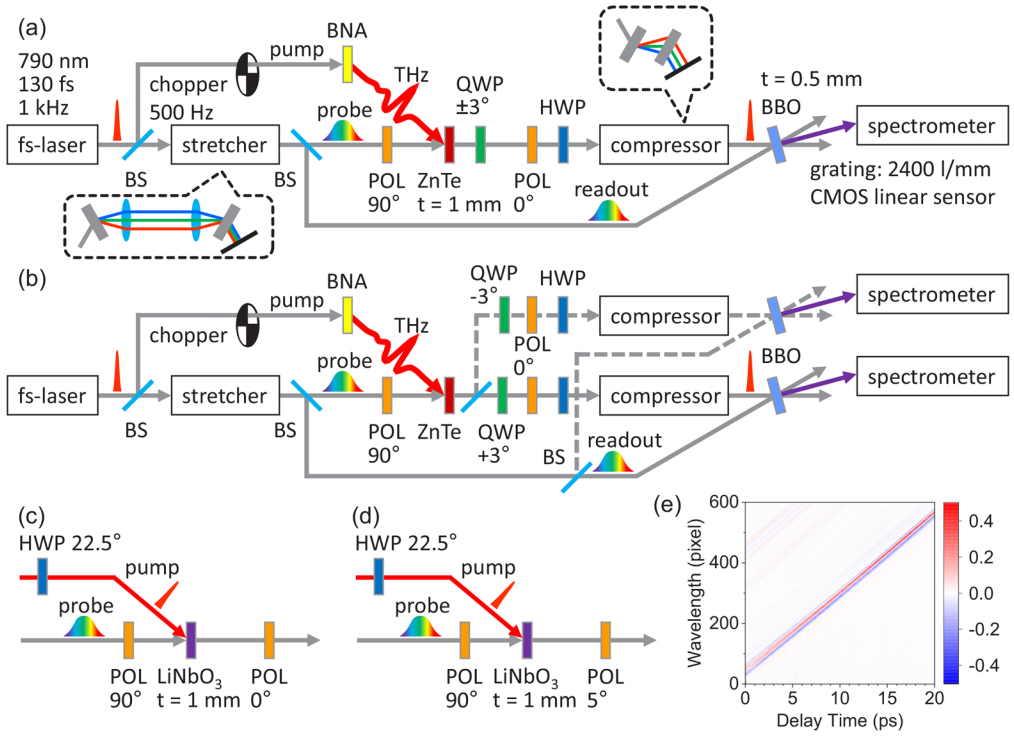

Fig. 3. (a,b) Experimental setup of chirped-pulse up-conversion spectroscopy for terahertz waveform detection. BNA: N-benzyl-2-methyl-4-nitroaniline. BBO: beta-barium borate. POL: polarizer. QWP: quarter-wave plate. HWP: half-wave plate. BS: beam splitter. Time-resolved signal encoded by (c) Kerr rotations, (d) heterodyne detection, and (a,b) phase-offset electro-optic sampling. (e) Terahertz modulation signals obtained by translating the delay time to ensure time–wavelength conversion of chirped-pulse up-conversion spectroscopy with dispersion compensation. The group delay dispersion (GDD) is 0.4 ps^2.

Kerr rotations and phonon-polariton oscillations were measured using a 1-mm-thick $LiNbO_3$ crystal. The pump-pulse polarization was set at 45° relative to the probe-pulse polarization along the c-axis of the $LiNbO_3$ crystal. As shown in Fig. 3(c) and (d), crossed-Nicols and

Optics EXPRESS

heterodyne configurations were used to detect the Kerr rotations and phonon-polariton oscillations, respectively. The modulation signal was obtained from the up-converted signal with and without pump irradiation. The spectra were measured on a single-shot basis by using a CMOS linear sensor and an optical chopper with 1 kHz and 500 Hz repetition, respectively. The time-to-spectral conversion ratio was calibrated by changing the relative delay of the pump and probe pulses. Figure 3(e) shows the terahertz modulation signal induced by using chirped pulses with an additive GDD of 0.4 ps^2 and by translating the delay stage for the terahertz pump pulses. In this configuration, 40 fs/pixel was obtained with a time window of ca. 20 ps.

3. Results and discussion

3.1. Terahertz waveform detection using phase offset EO sampling

Chirped-pulse up-conversion spectroscopy was applied for terahertz waveform detection using phase offset EO sampling, and the results are summarized in Fig. 4 for signals averaged over an accumulation time of 1 s (500 pulses). The up-converted terahertz-induced modulation signals without dispersion compensation are shown in Fig. 4(a), where the phase offset angle was set at ±3° by QWP rotation and the red and blue lines indicate positive and negative phase offset signals, respectively. Without dispersion compensation, there was significant waveform distortion due to spectral interference, but Fig. 4(b) shows that the waveform distortion was compensated by using dispersion compensation. In the current setup, the additive GDD of the modulated probe pulse was −0.4 ps^2 while that of the readout pulse was 0.4 ps^2, yielding the accurate waveform without distortion. If the additive GDD was not compensated completely, namely the GDD ≠ −0.4 ps^2, the time resolution was degraded, and then the waveform distortion appeared. The terahertz electric field was retrieved as follows [33,35],

$$\frac{I_{SFG}(+\theta,\Delta)-I_{SFG}(-\theta,\Delta)}{I_{SFG}(\theta,0)} = \frac{2\sin\Delta}{\sin 2\theta} \quad \text{and} \quad \Delta = \frac{2\pi d}{\lambda} n^3 r_{41} E_{THz}, \tag{1}$$

where Δ is the terahertz-induced phase modulation, θ is the phase offset angle applied by the QWP, λ is the probe wavelength, and d, n, and r_{41} are the thickness, refractive index, and EO coefficient of the ZnTe crystal, respectively. The results indicate the detection of distortion-free waveforms by chirped-pulse up-conversion spectroscopy.

As shown in Fig. 4(c) and (d), conventional stage scanning was used to confirm the accuracy of waveform retrieval and its Fourier spectrum. As can be seen, chirped-pulse up-conversion spectroscopy with dispersion compensation retrieved an accurate terahertz waveform comparable to that from conventional stage scanning. The temporal resolution is also comparable to conventional stage scanning. In this study, the GDD was compensated using a Treacy pulse compressor with a pair of gratings, but the higher-order dispersion could not be compensated. Nevertheless, the results show that chirped-pulse up-conversion spectroscopy with dispersion compensation can detect accurate terahertz waveforms on a single-shot basis.

For the results shown in Fig. 4, the positive and negative phase offset signals were measured alternately. However, to reduce the effects due to pulse-to-pulse fluctuation of the probe pulses, we also performed an experiment in which the positive and negative phase offset signals were measured simultaneously. To achieve this, a non-polarizing beam splitter was placed after the ZnTe crystal and before the QWP, and the QWP rotation angle was set at ±3° as shown in Fig. 3(b). Figure 5(a) shows a typical terahertz waveform obtained by single-shot measurement, and to assess the measurement accuracy, Fig. 5(b) shows a histogram for the peak electric field, for which a variation of ±30 V/cm was realized. The signal-to-noise ratio of a single-shot measurement was estimated to be 23 dB. Unlike previous numerical or analytical methods, the proposed method does not require sophisticated signal post-processing and so can usefully be applied to real-time terahertz waveform detection and analysis.

Optics EXPRESS

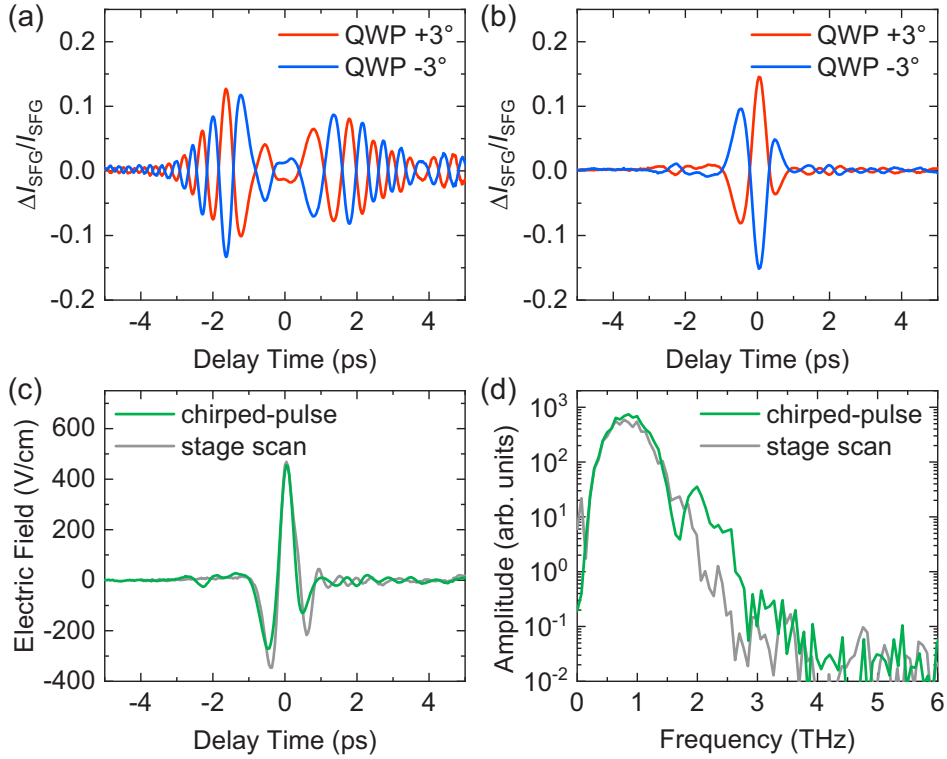

Fig. 4. Up-converted terahertz-induced modulation signals (a) without and (b) with dispersion compensation for positive (red) and negative (blue) phase offset angle. (c) Retrieved terahertz waveform with dispersion compensation (green), and waveform obtained by conventional stage scanning (gray). (d) Fourier spectrum for each method.

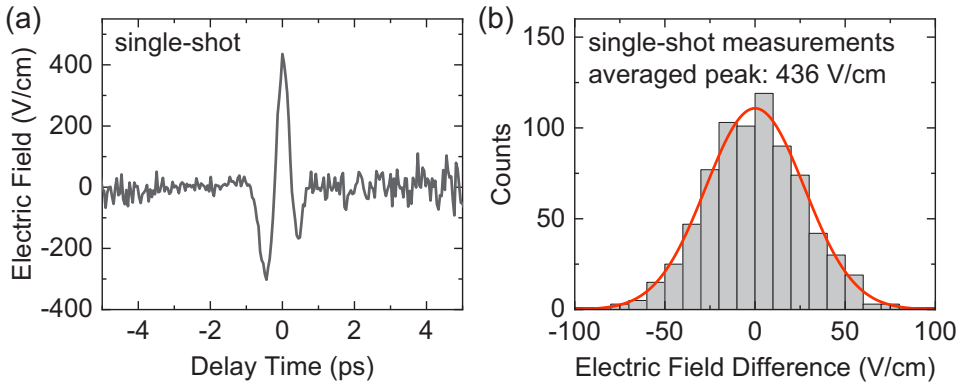

Fig. 5. (a) Single-shot terahertz electric-field waveform obtained by chirped-pulse up-conversion spectroscopy with dispersion compensation; the positive and negative phase offset signals were measured simultaneously in the phase offset EO sampling. (b) Histogram for peak electric field; an accuracy of ±30 V/cm was realized.

Optics EXPRESS

3.2. Kerr rotations and phonon-polariton oscillations of $LiNbO_3$

Kerr rotation signals of a $LiNbO_3$ crystal were obtained using chirped-pulse up-conversion spectroscopy with and without dispersion compensation. Note that the measurements were performed on a single-shot basis with a repetition rate of 1 kHz. Figure 6(a) shows the single-shot results for the up-converted modulation signal, and Fig. 6(b) shows the obtained signals averaged over an accumulation time of 1 s (500 pulses). As can be seen, an accurate time-domain signal was obtained with appropriate dispersion compensation (blue), whereas without dispersion compensation, there was significant waveform distortion (red) due to spectral interference. With dispersion compensation, the full width at half maximum of the Kerr rotation signal was 0.6 ps. We confirmed the Kerr rotation signal of 0.6 ps was also obtained even if we changed the additive GDD value as shown in Fig. 6(b), ensuring that the proposed method works well regardless of the amount of the chirped pulse width. In principle, the time resolution of the proposed method is limited by the transform-limited pulse width, and the slightly longer Kerr rotation signal corresponds to relaxation of the $LiNbO_3$ crystal. The results demonstrate sub-picosecond time-resolution in chirped-pulse spectroscopy with dispersion compensation.

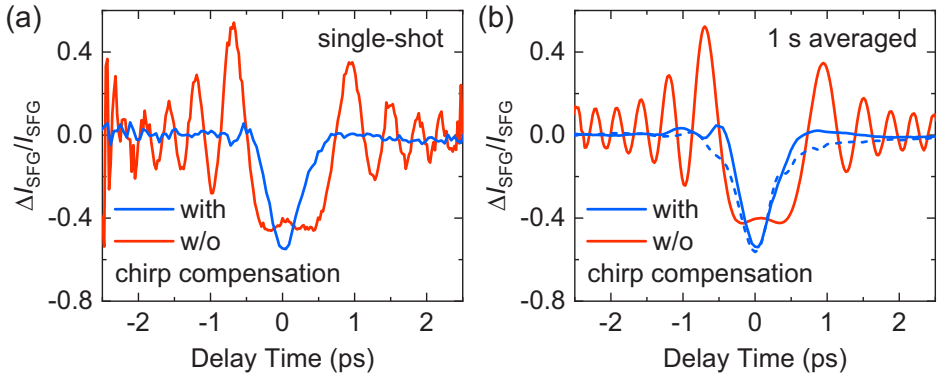

Fig. 6. Kerr rotation signal of $LiNbO_3$ crystal measured by chirped-pulse up-conversion spectroscopy with (a) single-shot measurement and (b) averaged over 500 pulses (1 s) with (blue) and without (red) dispersion compensation. The broken line in (b) indicates a twice as much additive GDD result with dispersion compensation.

An $LiNbO_3$ crystal has anisotropic phonon dispersion for the crystal axis [36], so phonon-polariton oscillations can be detected by means of a slight modification of the polarizers from the Kerr rotation measurements. Figure 7(a) shows the up-converted modulation signals of a $LiNbO_3$ crystal obtained under optical heterodyne configuration, where the output polarizer was rotated by 5° from the crossed-Nicols configuration as shown in Fig. 3(d). After the strong Kerr rotation signal at ca. 0 ps, successive terahertz-bandwidth oscillations are evident with the probe polarization parallel to either ordinary or extra-ordinary waves. As shown in Fig. 7(b), the corresponding Fourier spectra indicate peaks at 3 THz and 4 THz for ordinary and extra-ordinary waves, respectively. These oscillations originated from the E-mode phonon polaritons in $LiNbO_3$ with backward- and forward-propagating transverse optical modes [36]. The results indicate that chirped-pulse spectroscopy with dispersion compensation can observe terahertz-bandwidth oscillations.

Optics EXPRESS

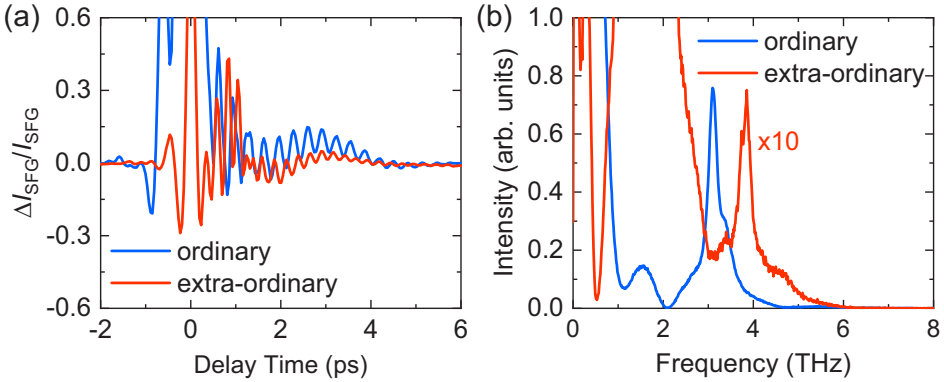

Fig. 7. (a) Terahertz-bandwidth oscillations of phonon-polariton modes of $LiNbO_3$ crystal measured by chirped-pulse up-conversion spectroscopy with dispersion compensation; the probe polarizations were ordinary (blue) and extra-ordinary (red) waves. (b) Fourier spectra.

4. Summary

We have demonstrated chirped-pulse up-conversion with dispersion compensation for ultrafast pump and probe spectroscopy with sub-picosecond time resolution on a single-shot basis. EO sampling and pump–probe spectroscopy experiments were conducted to measure terahertz waveforms, Kerr rotations, and phonon-polariton oscillations, with the temporal profile of the ultrafast signals encoded into the chirped pulses. By performing sum-frequency generation between the dispersion-compensated probe pulses and the chirped readout pulse, the time-domain signals could be observed accurately in the frequency domain without the significant distortion due to spectral interference that occurs in conventional chirped-pulse spectroscopy. The results show that chirped-pulse up-conversion spectroscopy with dispersion compensation can measure accurate ultrafast responses in the time domain as encoded in the chirped probe pulses with a time resolution corresponding to the transform-limited pulse width. Furthermore, the frequency-encoded time-domain signal can be transferred through an optical fiber, thereby allowing optical-fiber-based systems with compact and robust configurations to be established.

Funding. New Energy and Industrial Technology Development Organization (JPNP20004); Kanagawa Institute of Industrial Science and Technology; Japan Society for the Promotion of Science (JP20H05662, JP23K04623).

Disclosures. The authors declare no conflicts of interest.

Data availability. Data underlying the results presented in this paper are not publicly available at this time but may be obtained from the authors upon reasonable request.

References

1. P. R. Poulin and K. A. Nelson, "Irreversible organic crystalline chemistry monitored in real time," Science **313**(5794), 1756–1760 (2006).
2. K. Goda, K. K. Tsia, and B. Jalali, "Serial time-encoded amplified imaging for real-time observation of fast dynamic phenomena," Nature **458**(7242), 1145–1149 (2009).
3. G. Herink, B. Jalali, C. Ropers, *et al.*, "Resolving the build-up of femtosecond mode-locking with single-shot spectroscopy at 90 MHz frame rate," Nat. Photonics **10**(5), 321–326 (2016).
4. A. Mahjoubfar, D. V. Churkin, S. Barland, *et al.*, "Time stretch and its applications," Nat. Photonics **11**(6), 341–351 (2017).
5. J. Liang and L. V. Wang, "Single-shot ultrafast optical imaging," Optica **5**(9), 1113–1127 (2018).
6. Z. Chen, C. B. Curry, R. Zhang, *et al.*, "Ultrafast multi-cycle terahertz measurements of the electrical conductivity in strongly excited solids," Nat. Commun. **12**(1), 1638 (2021).
7. M. Kobayashi, Y. Arashida, K. Asakawa, *et al.*, "Pulse-to-pulse ultrafast dynamics of highly photoexcited $Ge_2Sb_2Te_5$ thin films," Jpn. J. Appl. Phys. **62**(2), 022001 (2023).
8. J. Takeda, W. Oba, Y. Minami, *et al.*, "Ultrafast crystalline-to-amorphous phase transition in $Ge_2Sb_2Te_5$ chalcogenide alloy thin film using single-shot imaging spectroscopy," Appl. Phys. Lett. **104**(26), 261903 (2014).

Optics EXPRESS

9. C. Evain, E. Roussel, M. Le Parquier, *et al.*, "Direct observation of spatiotemporal dynamics of short electron bunches in storage rings," Phys. Rev. Lett. **118**(5), 054801 (2017).
10. R. Tamaki, T. Kasai, G. Asai, *et al.*, "Pulse-to-pulse detection of terahertz radiation emitted from the femtosecond laser ablation process," Opt. Express **30**(13), 23622–23630 (2022).
11. J. Shan, A. S. Weling, E. Knoesel, *et al.*, "Single-shot measurement of terahertz electromagnetic pulses by use of electro-optic sampling," Opt. Lett. **25**(6), 426–428 (2000).
12. Y. Kawada, T. Yasuda, A. Nakanishi, *et al.*, "Single-shot terahertz spectroscopy using pulse-front tilting of an ultra-short probe pulse," Opt. Express **19**(12), 11228–11235 (2011).
13. K. S. Wilson and C. Y. Wong, "Single-shot transient absorption spectroscopy with a 45 ps pump-probe time delay range," Opt. Lett. **43**(3), 371–374 (2018).
14. G. P. Wakeham and K. A. Nelson, "Dual-echelon single-shot femtosecond spectroscopy," Opt. Lett. **25**(7), 505–507 (2000).
15. H. Sakaibara, Y. Ikegaya, I. Katayama, *et al.*, "Single-shot time-frequency imaging spectroscopy using an echelon mirror," Opt. Lett. **37**(6), 1118–1120 (2012).
16. Y. Minami, Y. Hayashi, J. Takeda, *et al.*, "Single-shot measurement of a terahertz electric-field waveform using a reflective echelon mirror," Appl. Phys. Lett. **103**(5), 051103 (2013).
17. T. Shin, J. W. Wolfson, S. W. Teitelbaum, *et al.*, "Dual echelon femtosecond single-shot spectroscopy," Rev. Sci. Instrum. **85**(8), 083115 (2014).
18. G. T. Noe, I. Katayama, F. Katsutani, *et al.*, "Single-shot terahertz time-domain spectroscopy in pulsed high magnetic fields," Opt. Express **24**(26), 30328–30337 (2016).
19. Z. Jiang and X. C. Zhang, "Single-shot spatiotemporal terahertz field imaging," Opt. Lett. **23**(14), 1114–1116 (1998).
20. M. Kobayashi, Y. Arashida, G. Yamashita, *et al.*, "Fast-frame single-shot pump-probe spectroscopy with chirped-fiber Bragg gratings," Opt. Lett. **44**(1), 163–166 (2019).
21. S. M. Teo, B. K. Ofori-Okai, C. A. Werley, *et al.*, "Invited Article: Single-shot THz detection techniques optimized for multidimensional THz spectroscopy," Rev. Sci. Instrum. **86**(5), 051301 (2015).
22. I. A. Shkrob, D. A. Oulianov, R. A. Crowell, *et al.*, "Frequency-domain 'single-shot' ultrafast transient absorption spectroscopy using chirped laser pulses," J. Appl. Phys. **96**(1), 25–33 (2004).
23. M. Kobayashi, Y. Minami, C. L. Johnson, *et al.*, "High-acquisition-rate single-shot pump-probe measurements using time-stretching method," Sci. Rep. **6**(1), 37614 (2016).
24. B. Yellampalle, K. Y. Kim, G. Rodriguez, *et al.*, "Algorithm for high-resolution single-shot THz measurement using in-line spectral interferometry with chirped pulses," Appl. Phys. Lett. **87**(21), 211109 (2005).
25. A. Tikan, S. Bielawski, C. Szwaj, *et al.*, "Single-shot measurement of phase and amplitude by using a heterodyne time-lens system and ultrafast digital time-holography," Nat. Photonics **12**(4), 228–234 (2018).
26. E. Roussel, C. Szwaj, C. Evain, *et al.*, "Phase Diversity Electro-optic Sampling: A new approach to single-shot terahertz waveform recording," Light: Sci. Appl. **11**(1), 14 (2022).
27. C. V. Bennett and B. H. Kolner, "Upconversion time microscope demonstrating 103× magnification of femtosecond waveforms," Opt. Lett. **24**(11), 783–785 (1999).
28. P. Suret, R. E. Koussaifi, A. Tikan, *et al.*, "Single-shot observation of optical rogue waves in integrable turbulence using time microscopy," Nat. Commun. **7**(1), 13136 (2016).
29. B. H. Kolner, "Active pulse compression using an integrated electro-optic phase modulator," Appl. Phys. Lett. **52**(14), 1122–1124 (1988).
30. R. Salem, M. A. Foster, A. C. Turner, *et al.*, "Signal regeneration using low-power four-wave mixing on silicon chip," Nat. Photonics **2**(1), 35–38 (2008).
31. H. Hashimoto, Y. Okada, H. Fujimura, *et al.*, "Second-harmonic generation from single crystals of N-substituted 4-nitroanilinnes," Jpn. J. Appl. Phys. **36**(11R), 6754–6760 (1997).
32. M. Shalaby, C. Vicario, K. Thirupugalmani, *et al.*, "Intense THz source based on BNA organic crystal pumped at Ti:sapphire wavelength," Opt. Lett. **41**(8), 1777–1780 (2016).
33. F. D. J. Brunner, J. A. Johnson, S. Grübel, *et al.*, "Distortion-free enhancement of terahertz signals measured by electro-optic sampling. I. Theory," J. Opt. Soc. Am. B **31**(4), 904–910 (2014).
34. J. A. Johnson, F. D. J. Brunner, S. Grübel, *et al.*, "Distortion-free enhancement of terahertz signals measured by electro-optic sampling. II. Experiment," J. Opt. Soc. Am. B **31**(5), 1035–1040 (2014).
35. G. Asai, D. Hata, S. Harada, *et al.*, "High-throughput terahertz spectral line imaging using an echelon mirror," Opt. Express **29**(3), 3515–3523 (2021).
36. T. Kuribayashi, T. Motoyama, Y. Arashida, *et al.*, "Anharmonic phonon-polariton dynamics in ferroelectric $LiNbO_3$ studied with single-shot pump-probe imaging spectroscopy," J. Appl. Phys. **123**(17), 174103 (2018).